Title

Siderophores provoke extracellular superoxide production by Arthrobacter strains during carbon sources-level fluctuation

Journal

Environmental Microbiology, 24(2)

ISSN

1462-2912

Authors

Ning, Xue
Liang, Jinsong
Men, Yujie
et al.

Publication Date

2022-02-01

DOI

10.1111/1462-2920.15914

environmental microbiology

Environmental Microbiology (2022) **24**(2), 894–904 doi:10.1111/1462-2920.15914

Siderophores provoke extracellular superoxide production by *Arthrobacter* strains during carbon sources-level fluctuation

Xue Ning[1] **Jinsong Liang**[2,3,4*] **Yujie Men**[5] **Yuhan Wang**[2] **Yangyang Chang**[6] **Yaohui Bai**[3] **Huijuan Liu**[1] **Aijie Wang**[2,3] **Tong Zhang**[4] **and Jiuhui Qu**[1,3*]

[1]*Center for Water and Ecology, Tsinghua University, Beijing, 100084, China.*

[2]*School of Civil and Environmental Engineering, Harbin Institute of Technology, Shenzhen, 518055, China.*

[3]*Key Laboratory of Drinking Water Science and Technology, Research Center for Eco-Environmental Sciences, Chinese Academy of Sciences, Beijing, 100085, China.*

[4]*Environmental Microbiome Engineering and Biotechnology Laboratory, The University of Hong Kong, Hong Kong SAR, China.*

[5]*Department of Chemical and Environmental Engineering, University of California, Riverside, CA, 92521.*

[6]*School of Environmental Science and Technology, Dalian University of Technology, Dalian, 116024, China.*

Summary

Superoxide and other reactive oxygen species (ROS) shape microbial communities and drive the transformation of metals and inorganic/organic matter. Taxonomically diverse bacteria and phytoplankton produce extracellular superoxide during laboratory cultivation. Understanding the physiological reasons for extracellular superoxide production by aerobes in the environment is a crucial question yet not fully solved. Here, we showed that iron-starving *Arthrobacter* sp. QXT-31 (*A.* QXT-31) secreted a type of siderophore [deferoxamine (DFO)], which provoked extracellular superoxide production by *A.* QXT-31 during carbon sources-level fluctuation. Several other siderophores also demonstrated similar effects to *A.* QXT-31. RNA-Seq data hinted that DFO stripped iron from iron-bearing proteins in electron transfer chain (ETC) of metabolically active *A.* QXT-31, resulting in electron leakage from the electron-rich (resulting from carbon sources metabolism by *A.* QXT-31) ETC and superoxide production. Considering that most aerobes secrete siderophore(s) and undergo carbon sources-level fluctuation, the superoxide-generation pathway is likely a common pathway by which aerobes produce extracellular superoxide in the environment, thus influencing the microbial community and cycling of elements. Our results pointed that the ubiquitous siderophore might be the potential driving force for the microbial generation of superoxide and other ROS and revealed the important role of iron physiology in microbial ROS generation.

Received 20 October, 2021; revised 15 January, 2022; accepted 17 January, 2022. *For correspondence. E-mail jhqu@tsinghua.edu.cn; Tel: +010-62849151; Fax: +010-62849151; E-mail liangjinsong@hit.edu.cn; Tel: +86-18565801115; Fax: +010-62849151.

Introduction

Reactive oxygen species (ROS) are ubiquitous in the freshwater (Vermilyea *et al*., 2010) and ocean system (Rose *et al*., 2008), and drive the environmental transformation of metals (Learman *et al*., 2011; Pi *et al*., 2019) and organic matter (Pullin *et al*., 2004; Li *et al*., 2014). The sources of environmental ROS include abiotic photooxidation of natural organic matter (Garg *et al*., 2011; Zhong *et al*., 2021), metabolism of phytoplankton (Diaz and Plummer, 2018; Plummeer *et al*., 2019) and heterotrophic bacteria (Shvinka *et al*., 1979; Diaz *et al*., 2013). The physiological significance of the microbial extracellular superoxide has been recently linked to bacterial growth regulation (Hansel *et al*., 2019) and phytoplankton photophysiology (Diaz *et al*., 2019). However, the physiological reasons for extracellular ROS production by phytoplankton and heterotrophic bacteria are far from clear. A better understanding of the physiological reasons for microbial production of extracellular ROS would help identify the influencing factors for microbial ROS production in natural ecosystems, and predict and regulate ROS's environmental occurrence.

To explore the physiological reasons for microbial ROS's environmental occurrence, survival challenges that aerobes would face in natural ecosystems have to be considered.

In contrast to laboratory cultivation, where abundant bioavailable nutrients are supplied to microbes, heterotrophic microorganisms in the environment face two non-negligible survival challenges: (i) carbon sources-level fluctuation. Microbes often suffer from carbon starvation in the natural environment (Roszak and Colwell, 1987). However, carbon sources frequently recover for environmental microbes. Soil microbes would obtain a higher concentration of carbon sources when the rain fell (Deng *et al*., 2017); rhizospheric microorganisms could obtain more carbon source from plant root exudates in the daytime than in the night (Zhai *et al*., 2013); heterotrophic aerobes in the upper ocean obtain more carbon source from phytoplankton exudates in the daytime than in the night (Fouilland *et al*., 2014). (ii) iron starvation. Iron in aerobic environments is commonly oxidized by oxygen into the ferric form (Fe(III)), which is insoluble at neutral pH, resulting in microbial iron starvation. To facilitate iron uptake, most aerobic and facultative anaerobic microorganisms synthesize and secrete at least one siderophore (Neilands, 1995), which are low-molecular-weight chelating agents with an extremely high affinity for ferric iron (Hider and Kong, 2010) and tend to accumulate in the environment due to their relatively good stability. Although environmental microorganisms often suffer from and respond to carbon sources-level fluctuation and iron starvation, the influence of the resultant physiological changes on microbial extracellular superoxide production has been rarely studied.

Here, we integrate bacterial cultivation, mass-spectrometry, and RNA-Seq to explore the mechanisms involved in extracellular superoxide production by a strain belonging to the widespread genus *Arthrobacter* under carbon sources-level fluctuation and iron-starved condition. The influence of carbon source-level fluctuation and bacterial extracellular secretions on extracellular superoxide production was explored collectively. We revealed that an *Arthrobacter* strain synthesizes and secretes one type of siderophores, deferoxamine (DFO), which accumulated extracellularly and provoke extracellular superoxide production by *Arthrobacter* strain during carbon sources-level fluctuation. This study shed light on the important role of bacterial physiological response to carbon sources-level fluctuation and iron starvation in the microbial extracellular superoxide production, thus inspired the potential application of siderophores on the regulation of microbial ROS production in the carbon sources-level-fluctuation environment.

Experimental procedures

Bacterial strain and cultivation

We used an aerobic gram-positive strain of *Arthrobacter* sp. QXT-31 (referred as *A*. QXT-31) isolated from surface soil obtained from a manganese mine in Hunan Province, China (Liang *et al*., 2016). The *A*. QXT-31 strain was deposited in the China General Microbiological Culture Collection Centre (CGMCC number 6631). For experimentation, *A*. QXT-31 was grown in a mineral salt medium (MSM, Supplementary Method S1), free of metal-chelator. For each cultivation in the liquid medium, an agar-plate colony was transferred into 30 ml of liquid culture for 48 h cultivation in the dark at 170 rpm and 30°C. After subculturing for one generation, the bacterial culture grown for 24 h was used as an inoculum (3% inoculation proportion, v:v). The other two *Arthrobacter* strains, *Arthrobacter cupressi* (CGMCC number 1.10783) and *Arthrobacter humicola* (CGMCC number 1.15654) were purchased from CGMCC for the experiment, and both were grown in modified peptone-yeast extract-glucose (mPYG) medium (Liang *et al*., 2016). Cell growth was estimated using optical density at 600 nm (OD_{600}) with the bacterial suspensions, monitored by a Spark™ 10 M microplate reader (Tecan, Switzerland).

Extracellular superoxide production assay

A superoxide-specific chemiluminescent (CL) probe (2-methyl-6-(4-methoxyphenyl)-3,7-dihydroimidazo[1,2-a] pyrazin-3(7H)-one (MCLA); TCI, Japan) was used for the extracellular superoxide assays (Godrant *et al*., 2009) using luminometer of the microplate reader above. According to our previous study (Liang *et al*., 2017), diethylene-triaminepentaacetic acid (DTPA; a kind of metal-chelator) was excluded in the superoxide quantification system. Xanthine and xanthine oxidase from bovine milk (Sigma-Aldrich, USA) were added to the bacterial cultures to generate a calibration curve between the superoxide production rate and superoxide CL signal intensity for calibration of the bacterial superoxide production rate (Godrant *et al*., 2009). Superoxide dismutase (SOD) from erythrocytes of *Bos grunniens* (Gansu Yangtaihe Biotechnology, China) was used to generate superoxide-free controls. Details are available in Supplementary Method S2.

Glucose quantification

Glucose concentration in the bacterial cultures was measured using a glucose quantification kit (E1010, Applygen, China) based on the glucose oxidase/peroxidase method (Trinder, 1969) following the manufacturer's instruction. A calibration curve between glucose concentration and optical density at 500 nm, which was determined using the microplate reader above, was established to calibrate the glucose concentration in samples.

Quantification of the reduced form of nicotinamide adenine dinucleotides

Intracellular NADH and extracellular superoxide were quantified in *A*. QXT-31 culture after sterile glucose re-supplementation. The 1 ml of glucose stock solution (6 g $\bullet L^{-1}$) was added into 60 ml of 3 day *A*. QXT-31 culture in a 150 ml Erlenmeyer flask to reach a final concentration of 100 mg$\bullet L^{-1}$, and then subject to shake cultivation. The 180 μl of the culture in triplicate was immediately transferred into a 96-well plate for extracellular superoxide quantification for 80 min using the luminometer of the microplate reader above. For intracellular NADH quantification, 8 ml of 3 day *A*. QXT-31 culture was collected into tubes at 0, 15, 30, 45, 60, and 75 min after glucose re-supplementation. The cultures were then centrifuged at 10 000 *g* and 4°C for 5 min to precipitate cells, and the cells pellet at the bottom of the tubes were washed twice with K_2HPO_4/KH_2PO_4 buffer (200 mM, pH 7.5) to remove the remaining media components. The cells were then resuspended with 1 ml of the buffer solution, transferred to a 2 ml centrifuge tube, and 0.25 ml of stainless-steel grinding beads with diameters of 2 mm were added. The cell was lysed by a sample grinder (Shanghai Jingxin Industrial Development; JXFSTPRP-4D) under the condition of 20 m s^{-1} for 270 s. The lysate was centrifuged at 10 000 *g* and 4°C for 5 min to collect supernatant, and a cycling assay for nicotinamide adenine dinucleotides (Matsumura and Miyachi, 1980) was used to quantify NADH in the supernatant.

Secretions fractionation and identification

Secretions of *A*. QXT-31 in MSM were fractionated based on molecular weight to explore the molecular weight range of the activated substance(s) facilitating superoxide production by *A*. QXT-31. Secretions in 48 h *A*. QXT-31 cultures were first centrifuged (Sigma 3-18KS, Germany) at 10 000 *g* and 4°C for 5 min, with the resulting supernatant filtrated through a 0.22 μm sterile filter (Guangzhou Jet Bio-Filtration, China) to prepare cell-free filtrate (CFF). The CFF was then fractionated into five fractions (>100 100–30, 30–10, 10–3, and <3 kDa) using Millipore ultrafiltration centrifugal filters with nominal molecular mass limits of 100, 30, 10, and 3 kDa. The 24 h *A*. QXT-31 cells were harvested by centrifugation (718 *g*, 30°C, 10 min) and suspended in each of the five fractions. The suspensions (180 μl) were added to microplate wells preloaded with MCLA (3.125 μM), glucose (50 mg$\bullet L^{-1}$), and SOD (120 kU$\bullet L^{-1}$, only for controls), and superoxide CL signal intensity was detected immediately. An Ultimate 3000 ultra-high-performance liquid chromatography system, combined with a Q Exactive Plus mass spectrometer (Thermo Fisher Scientific, USA), was used to identify the suspected substance(s) in the secretion fractions. Details are available in Supplementary Method S3.

Preparation of Fe(III)-saturated metal-chelators

Fe(III)-saturated metal-chelator solution was prepared by slowly adding freshly prepared Fe(III) solution ($FeCl_3{\cdot}6H_2O$ dissolved in deionized water) to the metal-chelator solution at a variable molar ratio (depending on Fe(III) complexing site number of metal-chelator molecules) so that the complexing site of each metal-chelator was saturated by Fe(III), leaving negligible uncomplexed Fe(III). The Fe(III)-preincubated metal-chelator solution was allowed to equilibrate for at least 1 h at room temperature before use.

RNA extraction, sequencing, and transcriptome analysis

RNA-Seq was used to estimate transcriptional abundance of *A*. QXT-31 cells in variable conditions: (i) *A*. QXT-31 cells cultured for 12, 24, 36, and 48 h with/without exogenetic DFO (2 μM) treatment; and (ii) 36-h *A*. QXT-31 cells treated by each of the four metal-chelators (2 μM; acetohydroxamic acid, ferrichrome, enterobactin, and deferrioxamine E) (please see the complete RNA-Seq data in Supporting Information Appendix S1). Each metal-chelator was added to the cultures (5 ml) in centrifuge tubes with a 0.22 μm hydrophobic membrane in the vent cap (Guangzhou Jet Bio-Filtration, China) to react with cells for 2 h in the dark at 170 rpm and 30°C. Cells in 0.5 ml of the culture (5 ml) were then harvested by centrifugation (10 000 *g*, 4°C, 3 min) at 0.5, 1, 1.5, and 2 h, with the four-cell samples collected at the four timepoints mixed thoroughly as an RNA-Seq sample. TRNzol reagent (DP424; TIANGEN, China) was used for RNA extraction according to the manufacturer's instruction, with modification of the cell lysis step, where cell pellets were pulverized by a pestle in liquid nitrogen (Liang *et al*., 2017). Extracted RNAs were kept at −80°C before cDNA library construction. Total RNA concentration, RNA integrity number (RIN), and RNA quality number (RQN) were evaluated using an Agilent 2100 Bioanalyzer (Santa Clara, USA). Samples with a RIN/RQN value above 8.0 were collected for sequencing. Sequencing was performed on a BGISEQ-500 sequencer by Beijing Genomic Institution (Shenzhen, China). The coding regions of all *A*. QXT-31 genes annotated by the NCBI Prokaryotic Genome Annotation Pipeline (Tatusova *et al*., 2016) (https://ftp.ncbi.nlm.nih.gov/genomes/all/GCF/001/969/265/GCF_001969265.1_ASM196926v1) were used as a reference for transcriptome analysis. Transcriptional abundance (fragments per kilobase transcript length per million fragments

mapped, FPKM) was estimated using a build-in script (*align_and_estimate_abundance.pl*) and normalized for cross-sample comparison using a build-in script (*abundance_estimates_to_matrix.pl*) with the Trinity platform (v2.8.5) (Haas *et al*., 2013).

Chemicals

Siderophores and siderophore analogues used in this study included acetohydroxamic acid (Rhawn, China, >98% purity); ferrichrome (*Ustilago sphaerogena*) (Sigma-Aldrich, >99%); enterobactin (*Escherichia coli*) (Sigma-Aldrich, ≥98%); and deferrioxamine E (Abcam, UK, >95%).

Statistical analysis

A two-tailed unpaired Student's *t*-test, Wilcoxon signed-ranks test, Friedman's test followed by post hoc Fisher's least significant difference test, and one-way ANOVA test followed by post hoc Tukey honest significant difference test were used for specific experiments. The statistical methods and sample sizes (*n*) are indicated in the legend of each figure; a probability value of $P < 0.05$ was considered significant; $^{**}P < 0.01$, $^{***}P < 0.001$; boxplots show the interquartile range, the horizontal lines show the median values, and the whiskers indicate the minimum-to-maximum range.

Accession numbers

All sequence data generated from RNA-Seq were deposited in the NCBI Sequence Read Archive database under accession number PRJNA607123.

Results and discussion

Glucose re-supplementation trigger extracellular superoxide production in culture

At first, we observed that no obvious extracellular superoxide was detected in 48 h *A*. QXT-31 cultures grown in liquid mineral salt medium (MSM; containing 250 mg•L^{-1} glucose as the sole carbon source and 1.78 μM $FeCl_3$; Supplementary Method S1), whereas sterile glucose re-supplementation (50 mg•L^{-1}) in 48 h *A*. QXT-31 cultures induced substantial superoxide production within approximate 30 min (Fig. 1A). After glucose was re-supplemented in the 48 h *A*. QXT-31 culture, the glucose concentration consistently decreased at first and then remained at a constant level (10 mg•L^{-1}); superoxide CL signal intensity initially increased and peaked when the glucose concentration reached the constant value and then persistently declined (Fig. 1A). Considering glucose re-supplementation could not induce superoxide production in the cell-free filtrate (CFF) of the 48 h *A*. QXT-31 culture (data not shown), the results above suggested that glucose metabolism by the 48 h *A*. QXT-31 cells resulted in extracellular superoxide production. Glucose of 50 mg•L^{-1} was then re-supplemented to *A*. QXT-31 cultures during 41 day cultivation, and results showed that glucose re-supplementation only provoked superoxide production in old (≥36 h) *A*. QXT-31 cultures (Fig. 1B) and maximal production rate in *A*. QXT-31 cultures after glucose re-supplementation peaked on the 6th day and then declined (Fig. 1B). These observations raised two questions: (i) what is the role of glucose in provoking superoxide production in old (≥36 h) *A*. QXT-31 cultures and (ii) why did glucose re-supplementation only trigger substantial superoxide production in old (≥36 h) *A*. QXT-31 cultures.

Superoxide was commonly generated via one-electron reduction of oxygen molecules, and respiration-dependent superoxide production varies with nutrient levels (McBee *et al*., 2017). Hence, we speculated that glucose triggers superoxide production in the culture by generating abundant electrons when metabolized by *A*. QXT-31. According to the speculation, the superoxide production rate would positively correlate with intracellular NADH content in the culture. The speculation was verified by results of superoxide and NADH quantification in 72 h *A*. QXT-31 culture after glucose re-supplementation. After glucose re-supplementation in 72 h *A*. QXT-31 culture, superoxide CL signal intensity fit perfectly (Pearson correlation coefficient $R = 0.968$) with the five NADH average concentrations values during the rising and declining stage (0–60 min) (Fig. 1C). Considering NADH is an important electron donor of the electron transport chain (ETC), the results suggested that glucose triggers superoxide production in the culture by generating abundant electrons when metabolized by *A*. QXT-31.

When passing along ETC, abundant electrons generated from glucose metabolism will not generate more superoxide unless it leaks prior to terminal oxidase of ETC. Electron leakage from the ETC of prokaryote was widely believed to enhance superoxide production (McBee *et al*., 2017). Hence, a portion of the electron generated from glucose metabolism was supposed to leak from ETC of old (≥36 h) *A*. QXT-31 cells. Considering glucose re-supplementation was unable to trigger superoxide production in young (<36 h) *A*. QXT-31 culture (Fig. 1B), there might exist other stimulative factors for electron leakage from the ETC in old (≥36 h) *A*. QXT-31 culture. The potential stimulative factors for electron leakage from the ETC have been explored in the following section.

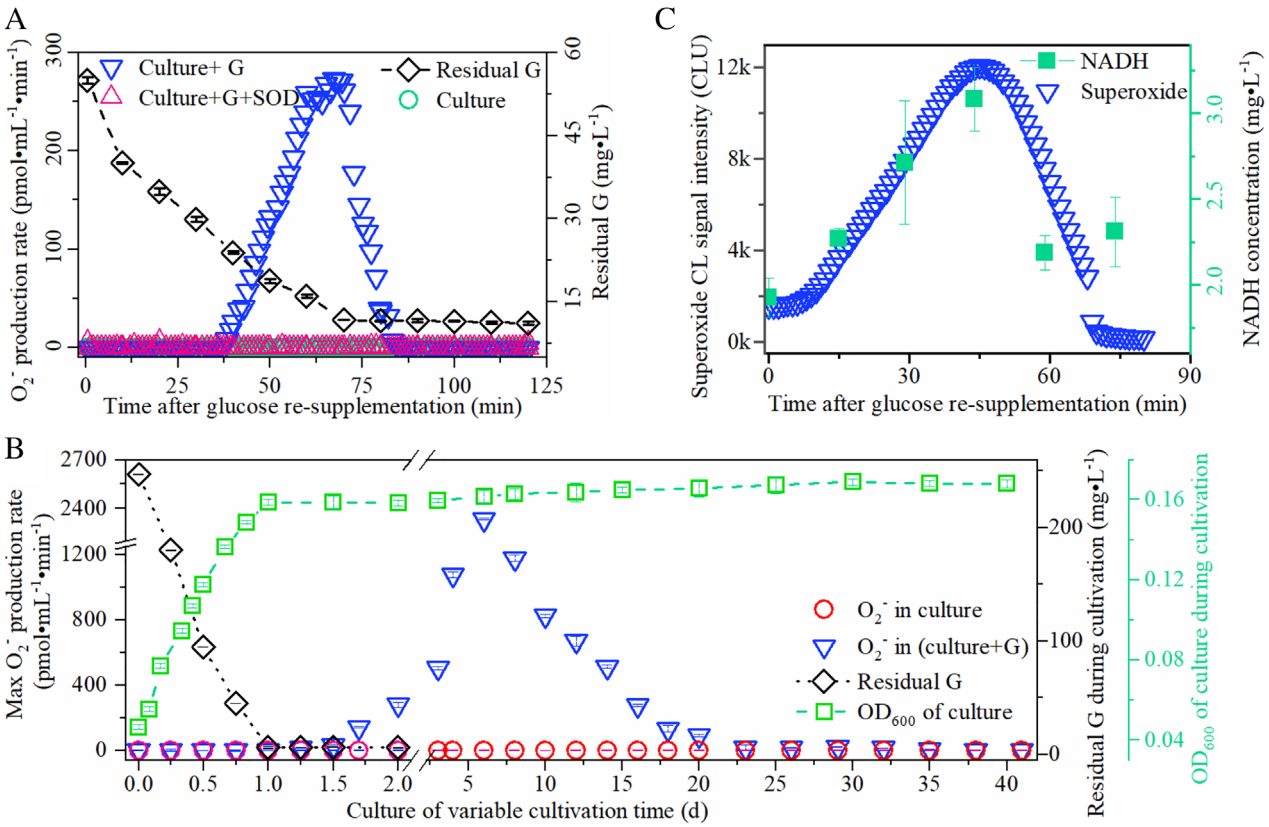

Fig. 1. Superoxide production in *A*. QXT-31 culture re-supplemented with different carbon sources.
A. Superoxide CL signal intensity (only one of three technological replicates is shown here, with the other two shown in Supplementary Fig. S1) and residual glucose concentration in 48 h *A*. QXT-31 cultures ($n = 3$) re-supplemented with/without sterile glucose (50 mg•L^{-1}). Superoxide was monitored on a microplate reader after 180 μl of culture was added to each prepared microplate well (reagents added in advance; $n = 3$). Wells with SOD (120 kU•L^{-1}) added were regarded as superoxide-free controls ($n = 3$).
B. Maximum superoxide production rate, residual glucose concentration, and optical density (OD_{600}) in *A*. QXT-31 cultures ($n = 3$) with/without sterile glucose re-supplementation (50 mg•L^{-1}) during 40 day cultivation.
C. Maximum superoxide production rate in 48 h *A*. QXT-31 cultures ($n = 3$) with/without re-supplementation of fructose, maltose, D-glucose, succinic acid, D-sucrose, malic acid, citric acid, pyruvic acid, acetic acid, or L-glucose. Carbon source re-supplementation in *A*. QXT-31 culture was consistent with carbon source upon which *A*. QXT-31 previously lived, except for L-glucose treatment, where L-glucose was supplemented to *A*. QXT-31 culture pre-grown in D-glucose. Each carbon source was re-supplemented at the same concentration of 50 mg•L^{-1}.
(A–C). Data are means ± SD. G, glucose.

The universality of extracellular superoxide production by Arthrobacter *strains*

Similar phenomena were also observed in the cultures of two other *Arthrobacter* strains (i.e. *A. cupressi* and *A. humicola*) grown in modified peptone-yeast extract-glucose (mPYG) medium (Liang *et al*., 2016) (Supplementary Fig. S2), suggesting the universality of superoxide production by *Arthrobacter* species during carbon sources-level fluctuation.

Glucose was not always available for the environmental microbe. Hence, we fed *A*. QXT-31 with various carbon sources (e.g. fructose, maltose, succinic acid, sucrose, malic acid, citric acid, pyruvic acid, acetic acid, and L-glucose). Then, we re-supplied the same carbon source to 48 h (stationary phase) *A*. QXT-31 cultures to explore the universality of superoxide production by *A*. QXT-31 during level fluctuation of various carbon sources. The results showed that when *A*. QXT-31 was grown in MSM with other metabolizable carbon sources, carbon source re-supplementation in the culture induced superoxide production; as expected, non-metabolizable L-isomer of glucose (L-glucose) was unable to induce the production of extracellular superoxide (Fig. 2). Considering that organic acids are harder to get through bacterial plasmalemma than sugars, it was not unexpected that sugars (e.g. glucose, fructose, maltose, sucrose) generally resulted to higher superoxide production rate than those organic acids (e.g. pyruvic acid, citric acid, succinic acid, malic acid, acetic acid). In addition, the carbon sources entering directly the TCA cycle (e.g. pyruvic acid, citric acid, succinic acid, malic acid) donor less electron than those sugars used even at the same intake mass. The relative high superoxide production rate of succinic

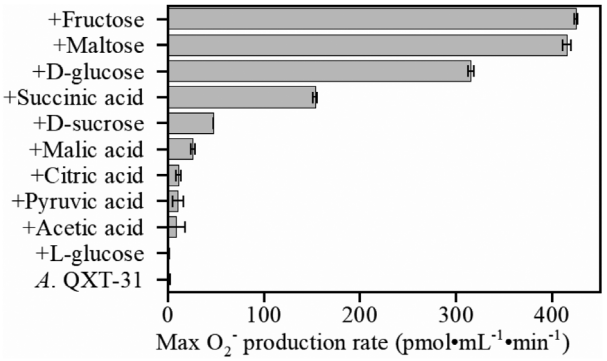

Fig. 2. Maximum superoxide production rate in 48 h *A*. QXT-31 cultures re-supplemented with fructose, maltose, D-glucose, succinic acid, D-sucrose, malic acid, citric acid, pyruvic acid, acetic acid, or L-glucose. Carbon source re-supplementation in *A*. QXT-31 culture ($n = 3$) was consistent with carbon source upon which *A*. QXT-31 previously lived, with the exception of L-glucose treatment, where L-glucose was supplemented to *A*. QXT-31 culture pre-grown in D-glucose. Each carbon source was re-supplemented at the same concentration of 50 mg•L^{-1}.

acid compared to other organic acids might derive from the possibility that succinic acid is direct electron donor for ETC complex II of *A*. sp. QXT-31, which is common for eukaryotic microorganisms. Based on the results above, we speculated the universality of extracellular superoxide production by *Arthrobacter* strains in the environment.

Extracellular secretions provoke extracellular superoxide production

It was noteworthy that glucose re-supplementation did not induce substantial extracellular superoxide production in young (<36 h) *A*. QXT-31 cultures (Fig. 1B). It was reasonable to speculate that cells and extracellular substances in old (≥36 h) *A*. QXT-31 cultures favoured superoxide production. As expected, when 24 h *A*. QXT-31 cells, deposited by centrifugation (718 *g*, 30°C, 10 min), were suspended with the cell-free filtrate (CFF) of 48 h *A*. QXT-31 culture, glucose re-supplementation induced superoxide production in the suspension (Fig. 3A; $P < 0.001$, two-tailed unpaired Student's *t*-test). These results demonstrated that extracellular substance(s) in 48 h *A*. QXT-31 culture induced 24 h cells to produce superoxide after glucose re-supplementation. The CFF of 48 h *A*. QXT-31 culture was then subjected to fractionation to explore the molecular weight range of the active substance(s), with five fractionations prepared (>100, 100–30, 30–10, 10–3, and <3 kDa). The <3 kDa CFF fraction in 48 h *A*. QXT-31 culture was the only fraction capable of triggering superoxide production by 24 h cells (Fig. 3B). The active substance(s) in <3 kDa CFF fraction was resistant to extreme pH (<4.0 and >10.0) and temperature (95°C) (data not shown). The active substance(s) characteristics in CFF were not consistent with that of most proteins, suggesting the possibility of a secondary metabolism product.

Extracellular deferoxamine provoke extracellular superoxide production

Liquid chromatography mass spectrometry (LC–MS) was used to separate and identify the active substance(s) in CFF. Chromatographic analysis of fresh MSM and <3 kDa CFF fractions of 24 and 48 h *A*. QXT-31 cultures showed that a conspicuous peak signal was only observed in the 24 and 48 h CFF, with the peak area in 48 h CFF approximately double that in 24 h CFF (Supplementary Fig. S3). The exclusive peak in CFF was then identified by electrospray ionization tandem mass spectrometry (ESI-MS/MS). Its primary and secondary mass spectra shared a predominant m/z peak and molecular ion fragmentation with deferoxamine (DFO) (Supplementary Fig. S4 and S5), a common type of microbial siderophore. The DFO standard (deferoxamine mesylate salt; European Pharmacopoeia Reference Standard) shared a similar retention time (12.51 min) as the exclusive peak in CFF (12.49 min) (Supplementary Fig. S3). The addition of 2.0 μM of DFO (approximate to the difference in DFO concentration between 24 and 48 h cultures) into glucose-re-supplemented 24, 36, and 48 h *A*. QXT-31 cultures significantly triggered/enhanced superoxide production (Fig. 3C; $P < 0.001$, two-tailed unpaired Student's *t*-test). A siderophore biosynthesis gene (locus tag BWQ92_RS08305) was predicted in the *A*. QXT-31 genome using the NCBI Prokaryotic Genome Annotation Pipeline (Tatusova *et al*., 2016) (website is provided in Methods section), indicating that *A*. QXT-31 is capable of synthesizing at least one type of siderophore. Our results strongly demonstrated that *A*. QXT-31 synthesized and secreted DFO during cultivation (probably as a responding to iron starvation), which accumulated extracellularly and provoked carbon-starving cells to produce superoxide when the utilizable carbon source was recovered.

The high affinity of DFO to Fe(III) is responsible for superoxide production

The affinity of DFO to Fe(III) under physiological conditions is much greater than that of the common artificial metal-chelator, ethylene diamine tetraacetic acid (EDTA) (Hider and Kong, 2010). Hence, it was hypothesized that DFO promotes superoxide production by exploiting its high affinity to Fe(III). The following experimental results supported this hypothesis: (i) each of the four other types

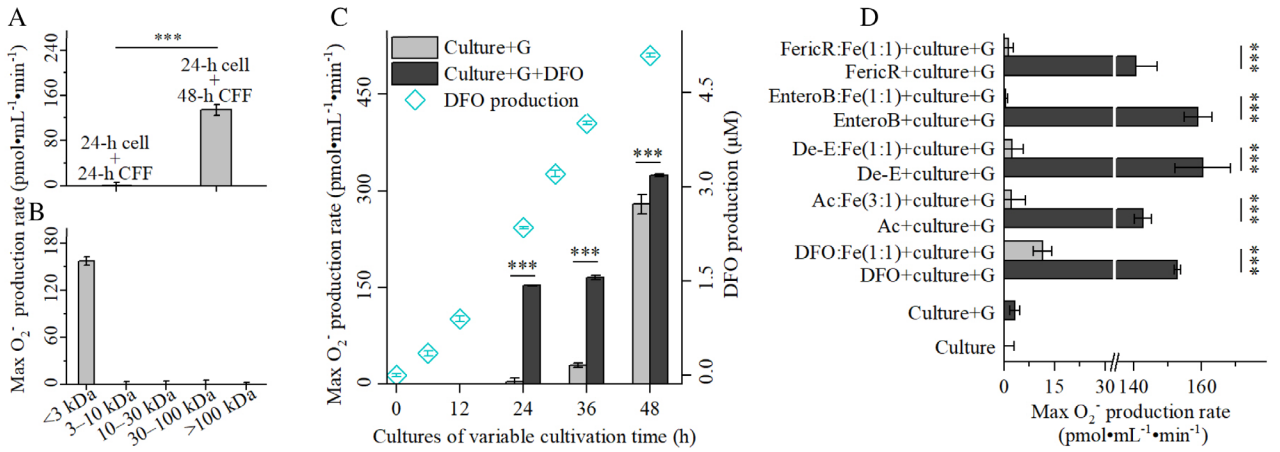

Fig. 3. DFO in CFF of *A*. QXT-31 culture provoked superoxide production.
A. Maximum superoxide production rate in 24 h *A*. QXT-31 culture and 24 h *A*. QXT-31 cell suspension in CFF of 48 h *A*. QXT-31 culture. Superoxide CL data were collected on a microplate reader after cultures/suspensions were mixed with 50 mg•L^{-1} glucose in microplate wells ($n = 3$).
B. Maximum superoxide production rate ($n = 3$) in 24 h *A*. QXT-31 cell suspension (with 50 mg•L^{-1} glucose re supplementation) in 48 h CFF fractions of <3, 3–10, 10–30, 30–100, and >100 kDa.
C. DFO production in *A*. QXT-31 cultures ($n = 3$), and maximum superoxide production rates in 24, 36, and 48 h cultures (with 50 mg•L^{-1} glucose re-supplementation, $n = 3$) with/without DFO addition (2 μM; approximate to DFO concentration in 24 h culture).
D. Maximum superoxide production rate in 24 h *A*. QXT-31 cultures (with/without 50 mg•L^{-1} glucose re-supplementation, $n = 3$) with/without each free/Fe(III)-saturated metal-chelator. FericR, ferrichrome; EnteroB, enterobactin; De-E, deferrioxamine E; Ac, acetohydroxamic acid. Data are means ± SD (A–D); *P* values were evaluated using a two-tailed unpaired Student's *t*-test (A, C and D); ***$P < 0.001$. G, glucose.

of iron-free metal-chelator (e.g. acetohydroxamic acid, deferrioxamine E, enterobactin, and ferrichrome) also triggered superoxide production in glucose-re-supplemented 24 h *A*. QXT-31 cultures (Fig. 3D); however, (ii) superoxide production was attenuated by pre-incubating the metal-chelators with Fe(III) (to prepare Fe(III)-saturated metal-chelator) (Fig. 3D; $P < 0.001$, two-tailed unpaired Student's *t*-test). Our finding is similar to a previous study, which demonstrated that some lectins (a group of proteins that bind specifically to certain sugars; natural source of lectins are most plants) would promote superoxide production by two red tide phytoplankton species (*Chattonella marina* and *Heterosigma akashiwo*), with the mechanism that lectins interact with carbohydrate moiety on the cell surface of the two phytoplankton species (Oda *et al*., 1998).

We repeated experiments with three Gram-positive bacteria (*Ensifer* sp., *Microbacterium* sp., *Bacillus* sp.) and three Gram-negative bacteria (*Escherichia coli*, *Pseudoxanthomonas* sp., *Pseudomonas* sp.) but found no obvious superoxide production in the cultures after the addition of glucose (50 mg•L^{-1}) and DFO (10 μM) during an 8 day cultivation (data not shown). The results suggested: (i) the possibility that only few aerobic bacterial populations are capable of producing superoxide during carbon level fluctuation, taking superoxide as a weapon for interspecies competition; (ii) the easier (compared to Gram-negative bacteria) contact between Gram-positive bacterial ETC and Fe-chelator by crossing only a permeable cell wall can only guarantee superoxide production during carbon level fluctuation for specific bacterial species.

DFO might disturb ETC function by stripping iron from ETC proteins

The underlying mechanism involved in the facilitation of superoxide production by DFO was further explored using RNA-Seq. Their high affinity for Fe(III) enables certain siderophores to strip iron from iron-bearing proteins (Wilson *et al*., 2016) and thus diminish their activities. Accordingly, DFO was suspected of stripping iron from iron-bearing proteins of *A*. QXT-31 and thus inactivating these proteins. RNA-Seq analysis showed that DFO supplementation (2.0 μM; approximate to DFO concentration in 24 h culture) up-regulated the transcriptional level of five genes encoding iron-related and iron-bearing proteins (including a Fe-S cluster assembly protein (locus tag BWQ92_21770), an NADH dehydrogenase (BWQ92_04045), two ubiquinol-cytochrome C reductases (BWQ92_20820 and BWQ92_20825), and a cytochrome B (BWQ92_20835)) in *A*. QXT-31 cultures at different ages (12, 24, 36, and 48 h) (Fig. 4A and Supplementary Table S1; $P < 0.01$ and 0.001, Wilcoxon signed-ranks test), and the highest upregulation of the five genes was observed in the 48 h culture (Fig. 4B and Supplementary Table S2; $P < 0.001$, Friedman's test), which might imply that cells were more vulnerable to higher

DFO concentration. Transcriptional upregulation of the same genes were also observed in 36 h *A*. QXT-31 cells treated by the other siderophores (2 μM), compared to cells without siderophore treatment (Fig. 4C; $P < 0.001$, Friedman's test). The highest transcriptional upregulation was observed in acetohydroxamic acid [its molecular weight (75 Da) and affinity to Fe(III) ($p^{Fe(III)} = 14.8$; $p^{Fe(III)}$ is defined as -log[$Fe^{(III)}$] where [$Fe^{(III)}$] represents the concentration of the free aqueous ion, [$Fe^{(III)}(H_2O)_6]^{3+}$] (Hider and Kong, 2010) are both lowest) treatments instead of enterobactin [its molecular weight (670 Da) and affinity to Fe(III) ($p^{Fe(III)} = 35.5$); Hider and Kong, 2010; are both highest] treatments (Fig. 4C; $P < 0.001$, Friedman's test), suggesting that the Fe(III)-affinity of acetohydroxamic acid was high enough to strip iron from the five proteins, and the small molecular size facilitated its physical contact with iron in proteins and thus iron stripping. An increase in Fe-S cluster synthesis could be a response to Fe-S cluster damage in proteins (Schwartz *et al*., 2001). Hence, the above results suggest that DFO stripped iron from these iron-bearing proteins (four of the five up-regulated genes encoded proteins of ETC) and thus impaired their activities. Specifically, the transcriptional upregulation of genes encoding NADH dehydrogenase (ETC complex I) and ubiquinol-cytochrome C reductase (ETC complex III) was observed after DFO addition (Fig. 4A; $P < 0.01$, Wilcoxon signed-ranks test), indicating that DFO caused the impairment/disfunction of the two complexes in the ETC of *A*. QXT-31 cells. Considering perturbations of ETC functions of eukaryotic cells promoted superoxide production during the consumption of NADH, the above results suggest that DFO-induced disfunction of electron-rich (resulting from carbon sources metabolism) ETC complexes I and III was a probable reason for superoxide production by metabolically active *A*. QXT-31.

Siderophores' role in microbial physiological ecology via provoking microbial superoxide production

The finding shed light on the important role of siderophores in microbial ecology. Aerobes produce and secrete over 500 different types of siderophores (Boukhalfa *et al*., 2003), which accumulate in the environment due to their good stability. Hydroxamate-type siderophores in soil have been reported as high as 10 μM (Plessner *et al*., 1993). In addition, aerobes often suffer from carbon level fluctuation in the environment (Hobbie and Hobbie, 2013). For example, soil microbes would obtain a higher concentration of carbon sources when the

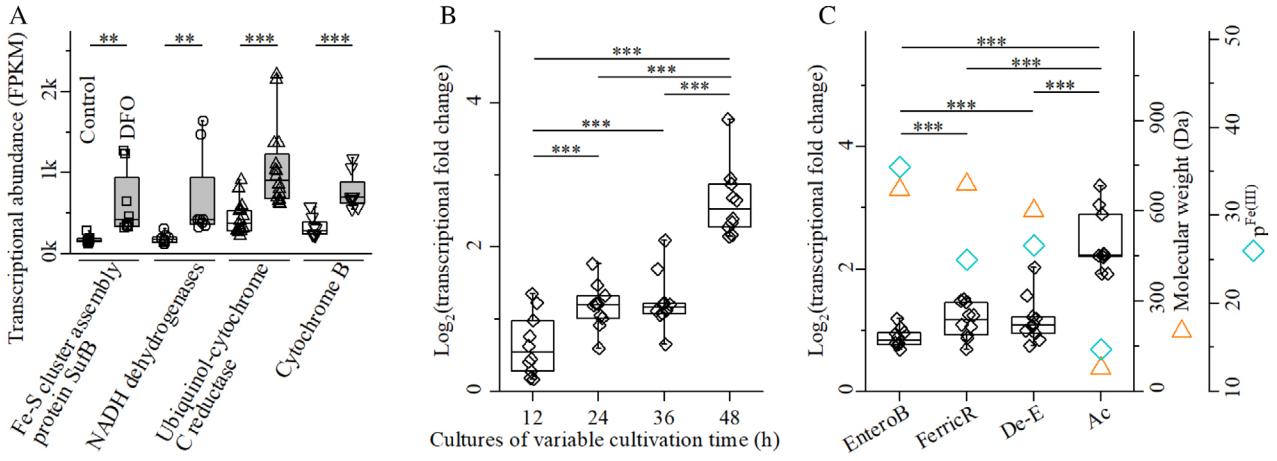

Fig. 4. Metal-chelators caused transcriptional upregulation of five genes encoding iron-related and iron-bearing proteins.
A. Changes in the transcriptional abundance (fragments per kilobase transcript length per million fragments mapped, FPKM) of five genes encoding iron-related and iron-bearing proteins (including a Fe-S cluster assembly protein (locus tag BWQ92_21770), an NADH dehydrogenase (BWQ92_04045), two ubiquinol-cytochrome C reductases (BWQ92_20820 and BWQ92_20825), and a cytochrome B (BWQ92_20835)) after 2.0 μM sterile DFO was added to 12, 24, 36 and 48 h *A*. QXT-31 cultures. DFO was added to the culture (5 ml) to react with cells for 2 h, and cells in 0.5 ml of the culture (5 ml) were then harvested by centrifugation (10 000 *g*, 4°C, 3 min) at 0.5 h, 1 h, 1.5 h, and 2 h, with the four cell samples collected at the four timepoints mixed thoroughly as an RNA-Seq sample. Cells in *A*. QXT-31 cultures without DFO addition were used as controls.
B. Comparison of DFO-inducing transcriptional fold change of the above genes in 12, 24, 36 and 48 h cultures.
C. Changes in the transcriptional abundance of the above five genes encoding iron-related and iron-bearing proteins in 36 h *A*. QXT-31 cultures ($n = 2$) after supplementation with (2 μM) acetohydroxamic acid (Ac), deferrioxamine E (De-E), enterobactin (EnteroB), and ferrichrome (FericR). RNA-Seq samples were prepared according to that of DFO. The molecular weights and pFe(III) values of the four types of metal-chelators are also shown for comparison, and pFe(III) is defined as -log[Fe(III)] where [Fe(III)] represents the concentration of the free aqueous ion, [Fe(III)$(H_2O)_6]^{3+}$. *P* values were evaluated using a Wilcoxon signed-ranks test (A), Friedman's test followed by post-hoc Fisher's least significant difference test (B and C); $^{**}P < 0.01$, $^{***}P < 0.001$; non-significant differences ($P \geq 0.05$) were not shown (B and C); the boxplots show the interquartile range, the horizontal lines show the median values, and the whiskers indicate the minimum-to-maximum range (A–C).

rain fell (Deng *et al*., 2017); rhizospheric microorganisms obtain more carbon source from plant root exudates in the daytime and less in the night time (Zhai *et al*., 2013); heterotrophic aerobes in the upper ocean obtain more carbon source from phytoplankton exudates in the daytime and less in the night time (Fouilland *et al*., 2014). When as low as 15 mg•L^{-1} of glucose became available for 48 h *A*. QXT-31 culture, obvious superoxide production was detected (Supplementary Fig. S7). Hence, when a small quantity of carbon becomes available for these Fe- and carbon-starving aerobes, some species (such as *Arthrobacter* species) of microflora are expected to produce extracellular superoxide. As superoxide and other ROS are toxic to cells, the neighbours of extracellular superoxide producers may be suppressed, and superoxide producers, which should be resistant to ROS, will likely succeed in carbon source competition. Hence, some aerobes may change the microbial community by producing extracellular superoxide when carbon source levels fluctuate. In addition, superoxide produced by Fe- and carbon-starving aerobes during carbon source fluctuation may also accelerate the environmental transformation of metals and inorganic/organic matter.

Considering superoxide capable of accelerating Fe uptake by aerobic organisms via reducing organically complexed Fe(III) to higher bioavailable Fe(II) (Garg *et al*., 2007), the physiology significance of siderophore-mediated superoxide production are readily apparent in light of facilitating microbial iron uptake in aerobic environment. Aerobic microorganisms increase Fe solubility via two main mechanisms, e.g. formation of organic complexes (such as siderophores) and reduction of Fe(III) to the more soluble Fe(II) state by Fe(III)-reducing regent (such as superoxide). Although biogenic superoxide was suggested to be a superior iron acquisition mechanism over organically complexes (such as siderophores) for certain marine phytoplankton (*Lyngbya majuscula*) due to superoxide's ability of non-specifically reducing various Fe(III) complexes to Fe(II) (Rose *et al*., 2005), our finding revealed that the two mechanisms could be intertwined in certain heterotrophic aerobes (e.g. *Arthrobacter* species). In view of the prevalence of superoxide production and siderophore synthesis by aerobic microorganisms, and two main iron-uptake mechanisms might also intertwine cross wide phylogeny (e.g. marine phytoplankton), and deserved to be considered.

Acknowledgements

This study was supported by the National Natural Science Foundation of China (31700106, 52170156, 51778603, and 51820105011) and the Shenzhen Science and Technology Program (grant no. KQTD20190929172630447). This research was also funded by the Hong Kong Scholars Program.

Author contributions

J.Q. and J.L. conceptualized the study. X.N., J.L., and Y.W. performed experiments and data analysis. J.L. and X.N. wrote the manuscript, with suggestions from Y.B., X.N., Y.M., T.Z., Y.C., H.L., and A.W.

References

Boukhalfa, H., Lack, J., Reilly, S.D., Hersman, L., and Neu, M.P. (2003) Siderophore production and facilitated uptake of iron and plutonium in P Putida. *AIP Conf Proc* **673**: 343–344.

Deng, Q., Hui, D., Chu, G., Han, X., and Zhang, Q. (2017) Rain-induced changes in soil CO2 flux and microbial community composition in a tropical forest of China. *Sci Rep-Uk* **7**: 5539.

Diaz, J.M., Hansel, C.M., Voelker, B.M., Mendes, C.M., Andeer, P.F., and Zhang, T. (2013) Widespread production of extracellular superoxide by heterotrophic bacteria. *Science* **340**: 1223–1226.

Diaz, J.M., and Plummer, S. (2018) Production of extracellular reactive oxygen species by phytoplankton: past and future directions. *J Plankton Res* **40**: 655–666.

Diaz, J.M., Plummer, S., Hansel, C.M., Andeer, P.F., Saito, M.A., and McIlvin, M.R. (2019) NADPH-dependent extracellular superoxide production is vital to photophysiology in the marine diatom Thalassiosira oceanica. *Proc Natl Acad Sci U S A* **116**: 16448–16453.

Fouilland, E., Tolosa, I., Bonnet, D., Bouvier, C., Bouvier, T., Bouvy, M., *et al*. (2014) Bacterial carbon dependence on freshly produced phytoplankton exudates under different nutrient availability and grazing pressure conditions in coastal marine waters. *FEMS Microbiol Ecol* **87**: 757–769.

Garg, S., Rose, A., and Waite, T. (2011) Photochemical production of superoxide and hydrogen peroxide from natural organic matter. *Geochim Cosmochim Acta* **75**: 4310–4320.

Garg, S., Rose, A.L., and Waite, T.D. (2007) Superoxide mediated reduction of organically complexed iron(III): comparison of non-dissociative and dissociative reduction pathways. *Environ Sci Technol* **41**: 3205–3212.

Godrant, A., Rose, A.L., Sarthou, G., and Waite, T.D. (2009) New method for the determination of extracellular production of superoxide by marine phytoplankton using the chemiluminescence probes MCLA and red-CLA. *Limnol Ocenogr* **7**: 682–692.

Haas, B.J., Papanicolaou, A., Yassour, M., Grabherr, M., Blood, P.D., Bowden, J., *et al*. (2013) De novo transcript sequence reconstruction from RNA-seq using the trinity platform for reference generation and analysis. *Nat Protocols* **8**: 1494–1512.

Hansel, C.M., Diaz, J.M., and Plummer, S. (2019) Tight regulation of extracellular superoxide points to its vital role in the physiology of the globally relevant Roseobacter clade. *MBio* **10**: 02668–02618.

Hider, R.C., and Kong, X. (2010) Chemistry and biology of siderophores. *Nat Prod Rep* **27**: 637–657.

Hobbie, J., and Hobbie, E. (2013) Microbes in nature are limited by carbon and energy: the starving-survival lifestyle in soil and consequences for estimating microbial rates. *Front Microbiol* **4**(00324): 1–11.

Learman, D.R., Voelker, B.M., Vazquez-Rodriguez, A.I., and Hansel, C.M. (2011) Formation of manganese oxides by bacterially generated superoxide. *Nat Geosci* **4**: 95–98.

Li, H.P., Daniel, B., Creeley, D., Grandbois, R., Zhang, S.J., Xu, C., *et al*. (2014) Superoxide production by a manganese-oxidizing bacterium facilitates iodide oxidation. *Appl Environ Microbiol* **80**: 2693–2699.

Liang, J., Bai, Y., Men, Y., and Qu, J. (2017) Microbe-microbe interactions trigger Mn(II)-oxidizing gene expression. *ISME J* **11**: 67–77.

Liang, J.S., Bai, Y.H., Hu, C.Z., and Qu, J.H. (2016) Cooperative Mn(II) oxidation between two bacterial strains in an aquatic environment. *Water Res* **89**: 252–260.

Matsumura, H., and Miyachi, S. (1980) Cycling assay for nicotinamide adenine dinucleotides. In *Methods in Enzymology*, San Pietro, A. (ed), (Vol. **69**, pp. 465–470). London, UK: Academic Press.

McBee, M.E., Chionh, Y.H., Sharaf, M.L., Ho, P., Cai, M.W. L., and Dedon, P.C. (2017) Production of superoxide in bacteria is stress- and cell state-dependent: a gating-optimized flow cytometry method that minimizes ROS measurement artifacts with fluorescent dyes. *Front Microbiol* **8**(459): 1–17.

Neilands, J.B. (1995) Siderophores: structure and function of microbial iron transport compounds. *J Biol Chem* **270**: 26723–26726.

Oda, T., Nakamura, A., Okamoto, T., Ishimatsu, A., and Muramatsu, T. (1998) Lectin-induced enhancement of superoxide anion production by red tide phytoplankton. *Mar Biol* **131**: 383–390.

Pi, K., Markelova, E., Zhang, P., and Van Cappellen, P. (2019) Arsenic oxidation by flavin-derived reactive species under oxic and anoxic conditions: oxidant formation and pH dependence. *Environ Sci Technol* **53**: 10897–10905.

Plessner, O., Klapatch, T., and Guerinot, M.L. (1993) Siderophore utilization by Bradyrhizobium japonicum. *Appl Environ Microbiol* **59**: 1688–1690.

Plummeer, S., Taylor, A.E., Harvey, E.L., Hansel, C.M., and Diaz, J.M. (2019) Dynamic regulation of extracellular superoxide production by the Coccolithophore Emiliania huxleyi (CCMP 374). *Front Microbiol* **10**(1546): 1–12.

Pullin, M.J., Bertilsson, S., Goldstone, J.V., and Voelker, B. M. (2004) Effects of sunlight and hydroxyl radical on dissolved organic matter: bacterial growth efficiency and production of carboxylic acids and other substrates. *Limnol Oceanogr* **49**: 2011–2022.

Rose, A.L., Salmon, T.P., Lukondeh, T., Neilan, B.A., and Waite, T.D. (2005) Use of superoxide as an electron shuttle for iron acquisition by the marine cyanobacterium Lyngbya majuscula. *Environ Sci Technol* **39**: 3708–3715.

Rose, A.L., Webb, E.A., Waite, T.D., and Moffett, J.W. (2008) Measurement and implications of non-photochemically generated superoxide in the equatorial Pacific Ocean. *Environ Sci Technol* **42**: 2387–2393.

Roszak, D.B., and Colwell, R.R. (1987) Survival strategies of bacteria in the natural environment. *Microbiol Rev* **51**: 365–379.

Schwartz, C.J., Giel, J.L., Patschkowski, T., Luther, C., Ruzicka, F.J., Beinert, H., and Kiley, P.J. (2001) IscR, an Fe-S cluster-containing transcription factor, represses expression of *Escherichia coli* genes encoding Fe-S cluster assembly proteins. *Proc Natl Acad Sci* **98**: 14895–14900.

Shvinka, J.E., Toma, M.K., Galinina, N.I., Skards, I.V., and Viesturs, U.E. (1979) Production of superoxide radicals during bacterial respiration. *J Gen Microbiol* **113**: 377–382.

Tatusova, T., DiCuccio, M., Badretdin, A., Chetvernin, V., Nawrocki, E.P., Zaslavsky, L., *et al*. (2016) NCBI prokaryotic genome annotation pipeline. *Nucleic Acids Res* **44**: 6614–6624.

Trinder, P. (1969) Determination of glucose in blood using glucose oxidase with an alternative oxygen acceptor. *Ann Clin Biochem* **6**: 24–27.

Vermilyea, A.W., Dixon, T.C., and Voelker, B.M. (2010) Use of (H_2O_2)-O-18 to measure absolute rates of dark H_2O_2 production in freshwater systems. *Environ Sci Technol* **44**: 3066–3072.

Wilson, B.R., Bogdan, A.R., Miyazawa, M., Hashimoto, K., and Tsuji, Y. (2016) Siderophores in iron metabolism: from mechanism to therapy potential. *Trends Mol Med* **22**: 1077–1090.

Zhai, X., Piwpuan, N., Arias, C.A., Headley, T., and Brix, H. (2013) Can root exudates from emergent wetland plants fuel denitrification in subsurface flow constructed wetland systems? *Ecol Eng* **61**: 555–563.

Zhong, J., Jiang, H., Wang, Z., Yu, Z., Wang, L., Mueller, J. F., and Guo, J. (2021) Efficient photocatalytic destruction of recalcitrant micropollutants using graphitic carbon nitride under simulated sunlight irradiation. *Environ Sci Ecotechnol* **5**: 1–11.

Supporting Information

Additional Supporting Information may be found in the online version of this article at the publisher's web-site:

Supplementary Fig. 1. Superoxide CL signal intensity in 48 h *A*. QXT-31 cultures re-supplemented with/without sterile glucose. **a** and **b** are results of other technological replicates of Fig. 1a. G: Glucose. SOD: superoxide dismutase.

Supplementary Fig. 2. Superoxide detection in cultures of two *Arthrobacter* strains after glucose re-supplementation. After glucose re-supplementation (50 mg•L^{-1}), superoxide CL signal intensity was determined in (**a**) 4 d *A*. *cupressi* culture and (**b**) 24 h *A. humicola* culture. Both strains were grown in mPYG medium. Only one of three technological replicates is shown here. G: Glucose.

Supplementary Fig. 3. Chromatograms of MSM, <3 kDa CFF fractions in 24 and 48 h *A*. QXT-31 cultures and 15.23 μM of DFO standard.

Supplementary Fig. 4. Comparison of primary electrospray ionization mass spectrogram between suspected chromatographic peak of <3 kDa CFF fraction in 48 h *A*. QXT-31 culture and DFO standard (15.23 μM) under positive (+p) and negative (−p) ionization modes.

Supplementary Fig. 5. Comparison of electrospray ionization secondary mass spectrogram between suspected chromatographic peak of <3 kDa CFF fraction in 48 h *A*. QXT-31 culture and DFO standard (15.23 μM) under positive (+p) and negative (−p) ionization modes.

Supplementary Fig. 6. Superoxide CL signal intensity in glucose-re-supplemented 24 h *A*. QXT-31 culture and suspension of DTPA-treated 24 h *A*. QXT-31 cells. **a** and **b** are results of other technological replicates of Fig. 4b. G: Glucose. SOD: superoxide dismutase.

Supplementary Fig. 7. Superoxide CL signal intensity in 48 h *A*. QXT-31 culture after glucose supplementation at various concentrations. Superoxide was monitored on a microplate reader after 180 μl of culture was added to each prepared microplate well (reagents added in advance).

Supplementary Table 1. Transcriptional abundance of five *A*. QXT-31 genes encoding iron-related and iron-bearing proteins after DFO addition. Transcriptional abundance was estimated using the metric of fragments per kilobase transcript length per million fragments mapped (FPKM).

Supplementary Table 2. Transcriptional abundance fold changes of five *A*. QXT-31 genes encoding iron-related and iron-bearing proteins after DFO addition. Data are expressed as the log2 fold change.

Appendix S1. Supporting Information.